Cell Death and Differentiation (2007) 14, 775–784

www.nature.com/cdd

Apoptosis-inducing factor is a major contributor to neuronal loss induced by neonatal cerebral hypoxia-ischemia

C Zhu[1,2], X Wang[1,2], Z Huang[1,2], L Qiu[1,2], F Xu[1,2], N Vahsen[3], M Nilsson[1], PS Eriksson[1], H Hagberg[1,4], C Culmsee[5], N Plesnila[6], G Kroemer[3] and K Blomgren[1,7]

Nine-day-old harlequin (Hq) mice carrying the hypomorphic apoptosis-inducing factor (AIF)^{Hq} mutation expressed 60% less AIF, 18% less respiratory chain complex I and 30% less catalase than their wild-type (Wt) littermates. Compared with Wt, the infarct volume after hypoxia-ischemia (HI) was reduced by 53 and 43% in male (YX^{Hq}) and female ($X^{Hq}X^{Hq}$) mice, respectively ($P < 0.001$). The Hq mutation did not inhibit HI-induced mitochondrial release of cytochrome *c* or activation of calpain and caspase-3. The broad-spectrum caspase inhibitor quinoline-Val-Asp(OMe)-CH_2-PH (Q-VD-OPh) decreased the activation of all detectable caspases after HI, both in Wt and Hq mice. Q-VD-OPh reduced the infarct volume equally in Hq and in Wt mice, and the combination of Hq mutation and Q-VD-OPh treatment showed an additive neuroprotective effect. Oxidative stress leading to nitrosylation and lipid peroxidation was more pronounced in ischemic brain areas from Hq than Wt mice. The antioxidant edaravone decreased oxidative stress in damaged brains, more pronounced in the Hq mice, and further reduced brain injury in Hq but not in Wt mice. Thus, two distinct strategies can enhance the neuroprotection conferred by the Hq mutation, antioxidants, presumably compensating for a defect in AIF-dependent redox detoxification, and caspase inhibitors, presumably interrupting a parallel pathway leading to cellular demise.
Cell Death and Differentiation (2007) **14,** 775–784. doi:10.1038/sj.cdd.4402053; published online 13 October 2006

Cell death involving a cell-autonomous active contribution of catabolic enzymes, apoptosis, plays a prominent role in the evolution of hypoxic-ischemic (HI) injury in the neonatal brain, and apoptosis is at least as important for the loss of neurons as unregulated cell death, necrosis.[1–3] Caspases are a class of specific cysteine proteases that mediate apoptotic death in a variety of cellular systems. Caspases are activated after HI, in particular in the immature brain.[2,3] The molecular pathway leading to caspase activation is initiated by mitochondrial outer membrane permeabilization (MOMP), presumably as a result of the permeability transition[4,5] and/or a process regulated by proteins from the Bcl-2 family.[6,7] MOMP results in the release of cytochrome *c* from the mitochondrial intermembrane space to the cytosol, where cytochrome *c* can interact with Apaf-1, triggering the formation of the apoptosome, the caspase-9 and caspase-3 activation complex. Prevention of caspase activation or inhibition of caspases affords neuroprotective effects in the immature brain.[8,9] Recent data demonstrate that when caspase activation is inhibited at or downstream of the apoptosome, neurons can undergo a delayed, caspase-independent death.[10,11] One of the key components of the caspase-independent cell death pathway is apoptosis-inducing factor (AIF).[12–14]

AIF has a dual function in the control of stress-induced cell death.[15] AIF is a phylogenetically old mitochondrial NADH oxidase whose local redox function is essential for optimal oxidative phosphorylation and for an efficient anti-oxidant defense. The absence of AIF can cause degeneration of cerebellar granule neurons and retinal ganglion cells, as has been shown for harlequin (Hq) mice. In the Hq mouse strain, the expression of AIF is reduced to approximately 20% of the wild type (Wt) level owing to a retroviral insertion into the first intron of the AIF gene located on chromosome X (AIF^{Hq}).[16,17] Hq mice develop ataxia owing to cerebellar atrophy as well as blindness owing to retinal degeneration.[17] In Hq mutant mice, lipid hydroperoxides were increased in both brain and cerebellum, indicative of increased oxidative stress, and this increase was more pronounced in older mice.[17] Cultured cerebellar granule neurons from Hq mice were more susceptible to peroxide-induced death, and transduction with Wt *aif* rescued this peroxide sensitivity.[17] The molecular

[1]Institute of Neuroscience and Physiology, Göteborg University, Göteborg, Sweden; [2]Department of Pediatrics, The Third Affiliated Hospital of Zhengzhou University, Zhengzhou, China; [3]Centre National de la Recherche Scientifique, FRE 2939, Institut Gustave Roussy, Villejuif, France; [4]Department of Obstetrics and Gynecology, Sahlgrenska University Hospital, Göteborg, Sweden; [5]Department of Pharmacy, Pharmaceutical Biology and Biotechnology, University of Munich, Munich, Germany; [6]Laboratory of Experimental Neurosurgery, Department of Neurosurgery and Institute for Surgical Research, University of Munich Medical Center – Grosshadern, Munich, Germany and [7]Department of Pediatric Oncology, The Queen Silvia Children's Hospital, Göteborg University, Göteborg, Sweden
Corresponding author: C Zhu, Institute of Neuroscience and Physiology, Göteborg University, Box 432, SE 405 30 Göteborg, Sweden. Tel: +46 31 773 3339; Fax: +46 31 773 3401; E-mail: changlian.zhu@neuro.gu.se
Keywords: caspase inhibitor; harlequin; oxidative stress; edaravone; free radical
Abbreviations: 4-HNE, 4-hydroxy-2-nonenal; AIF, apoptosis-inducing factor; AMC, aminomethylcoumarin; HI, hypoxia-ischemia; Hq, harlequin; MAP2, microtubule-associated protein-2; MOMP, mitochondrial outer membrane permeabilization; PBS, phosphate-buffered saline; Q-VD-OPh, quinoline-Val-Asp(OMe)-CH_2-PH; SOD1, Zn, Cu-superoxide dismutase; SOD2, Mn-superoxide dismutase; Wt, wild type
Received 11.7.06; revised 04.9.06; accepted 13.9.06; Edited by L Green; published online 13.10.06

etiology of this enhanced susceptibility to oxidative stress might involve a defect in oxidative phosphorylation[18] and/or in the redox activity of AIF.[17] Nonetheless, AIF has also been implicated in neuronal apoptosis as a cell death effector. In several models of apoptosis, AIF translocates to the nucleus, where it induces chromatin condensation and DNA degradation.[16,19–22] The nuclear translocation of AIF can be inhibited by blocking upstream signals of apoptosis (such as poly(ADP-ribose) polymerase-1),[16,23] inhibition of non-caspase cysteine proteases that are involved in the detachment of AIF from the inner mitochondrial membrane,[24] suppression of MOMP[21] or overexpression of heat-shock protein 70, which can intercept AIF in the cytosol.[25,26]

Both in neonatal HI and in adult focal ischemia, AIF translocates to nuclei during post-ischemic cell death, correlating with signs of DNA damage in the affected nuclei.[19,20] A few studies have confirmed a relative resistance of AIF-negative cells to apoptosis induction as compared to AIF-positive cells, in particular apoptosis induction pathways. Microinjection of AIF-neutralizing antibodies can reduce the neurotoxic effects of NMDA in primary murine cortical cultures.[27] Knock down of AIF with small interfering RNAs (siRNAs) protects primary cultures of hippocampal neurons and HT22 cells from glutamate toxicity[16] and differentiated PC12 cells against the neurotoxin 1-methyl-4-phenylpyridinium.[28] *In vivo* excitotoxic studies using kainic acid-induced seizures revealed that Hq mice had significantly less hippocampal damage than Wt littermates.[13] In addition, the brains of adult Hq mice are particularly resistant to focal ischemia.[16]

The aim of this study was to follow up our previous findings on AIF translocation after neonatal cerebral HI[19] and to develop therapeutic strategies based on the reduction of AIF expression. We demonstrate that the neuroprotective effects of the Hq mutation can be greatly enhanced by simultaneous scavenging of reactive oxygen species or by inhibition of caspases.

Results

Impact of the Hq mutation on the immature brain under physiological conditions. The total amount of AIF protein was reduced by a factor of 2.5 in male (YX^{Hq}) and female ($X^{Hq}X^{Hq}$) mice carrying the Hq mutation, as compared to age-matched (P9) Wt control mice (Figure 1a and b). This

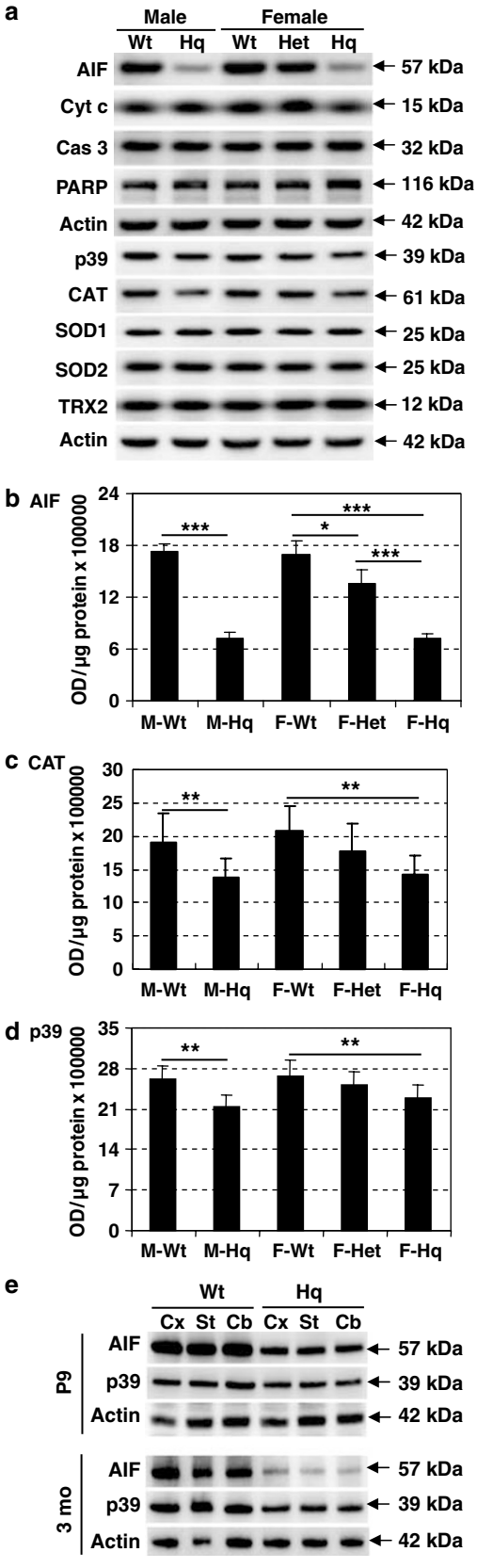

Figure 1 Expression of some apoptosis- and oxidative stress-related proteins in P9 Wt and Hq mouse brains. (**a**) Western blots of cortex homogenates from Wt and Hq mutant male and female mice, including female heterozygous (Het) mice ($n = 6$/group). The levels of cytochrome *c* (Cyt *c*), caspase-3 (Cas 3), poly(ADP-ribose) polymerase (PARP), OxPhos complex I 39 kDa subunit (p39), catalase (CAT), superoxide dismutase-1 (SOD1), superoxide dismutase-2 (SOD2) and TRX2. Onlyp39 and catalase were significantly different. Actin was used for control of equal loading. (**b**) Densitometric quantification of AIF expression. (**c**) Densitometric quantification of catalase expression. (**d**) Densitometric quantification of p39 expression. (**e**) Pooled samples of homogenates from Wt and Hq cortex (Cx), striatum (St) and cerebellum (Cb) from neonatal, P9 and adult, 3-month-old (3 mo) mice. Results are shown as means ± S.E.M. of six independent determinations. $^{*}P < 0.05$, $^{**}P < 0.01$, $^{***}P < 0.001$

correlated with a reduction in the *aif* transcript by a factor of ~9, as determined by microarray analysis (Supplementary Table 1). The brains of post-natal day 9 (P9)–P12 Hq mice exhibited a normal ultrastructure, and Hq mice manifested normal behavior at this age, in accordance with the fact that the Hq-associated neurodegeneration manifests much later, usually at >10 weeks of age.[17] Accordingly, the metabolic blood parameters of Hq mice were normal on P9 (Supplementary Table 2). The vascular anatomy of Hq mice does not differ from Wt mice.[16] The brains from Hq mice revealed relatively mild changes in the overall transcriptome, with no dramatic changes in the overall abundance of redox-active transcripts (Supplementary Table 1) apart from peroxiredoxin and catalase that were downregulated (Supplementary Table 1). Accordingly, P9 Hq brains contained reduced catalase protein (by ~30%, Figure 1a and c), yet normal levels of anti-oxidant stress proteins such as superoxide dismutases (Zn, Cu-superoxide dismutase (SOD1) and Mn-superoxide dismutase (SOD2)) and thioredoxin 2 (TRX2) (Figure 1a). P9 Hq mice exhibited a mild reduction in the abundance of the respiratory chain subunits, such as the p39 subunit of complex I (Figure 1a and d), which was less pronounced than in adult mice (Figure 1e). Furthermore, although the amount of AIF protein was reduced by a factor of 2.5 in the Hq brains of P9 mice, it was further reduced, by a factor 4.0, in 3-month-old Hq compared with Wt mice, and the levels were the same in the cortex, striatum and cerebellum (Figure 1e).

Impact of the Hq mutation on the immature brain after HI

Tissue loss and neuropathological scores were reduced in male and female Hq mice. Brain injury was evaluated on P12, after 72 h of reperfusion after HI. At this time point, the infarcts can be clearly delineated using microtubule-associated protein-2 (MAP2) staining[3] (Figure 2a). The total infarct volume in male Hq mutant mice ($6.55 \pm 0.99\,mm^3$, $n=37$) was reduced by 52.6% ($P=0.0011$) as compared with male Wt control mice ($13.82 \pm 1.86\,mm^3$, $n=33$)

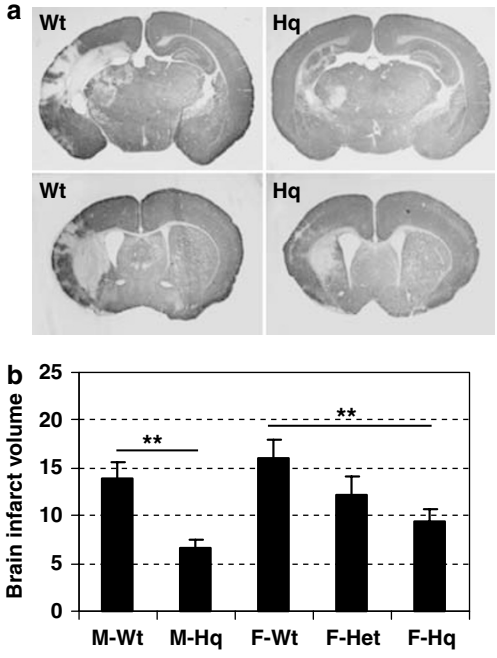

c

Groups	No.	Cortex	Hippocampus	Striatum	Thalamus	Total
M-Wt	n = 33	2.04 ± 0.22	3.64 ± 0.24	3.75 ± 0.31	2.60 ± 0.25	12.0 ± 0.93
M-Hq	n = 37	1.29 ± 0.20*	2.61 ± 0.23**	3.37 ± 0.27	1.90 ± 0.24*	9.17 ± 0.90*
F-Wt	n = 29	2.60 ± 0.24	4.25 ± 0.25	4.44 ± 0.31	2.85 ± 0.28	14.1 ± 1.04
F-Het	n = 36	1.81 ± 0.26*	3.51 ± 0.26*	3.96 ± 0.27	2.62 ± 0.24	11.9 ± 0.97
F-Hq	n = 31	1.56 ± 0.21**	3.12 ± 0.23**	3.19 ± 0.24**	2.31 ± 0.19	10.2 ± 0.82**

Figure 2 Brain injury after HI in Wt and Hq mutant mice. (**a**) Representative MAP2 stainings 72 h post-HI. Brain sections obtained at the dorsal hippocampus level (upper panels) and striatum level (bottom panels) for both Wt (left panels) and Hq mutant mice (right panels) are shown. Brain injury was evident in the cortex, striatum, hippocampus and thalamus, more pronounced in the Wt than Hq mutant mice. (**b**) Infarct volumes, as determined by MAP2 stainings. The total infarct volume was reduced by 52.6% in male Hq mutant mice ($n=37$) as compared with male Wt mice ($n=33$). In the females, the infarct volume was reduced by 41.0% in Hq mutants ($n=31$) and 22.7% in heterozygotes ($n=36$) as compared with Wt females ($n=29$). (**c**) Neuropathological scores in distinct brain regions. Data presented represent the mean ± S.E.M. $^*P<0.05$, $^{**}P<0.01$

(Figure 2b). The infarct volume was also reduced by 41.0% ($P=0.006$) in female Hq mutants ($9.5\pm1.3\,mm^3$, $n=31$) and 22.7% ($P=0.112$, NS) in heterozygous females ($12.1\pm1.9\,mm^3$, $n=36$), as compared with the Wt control mice ($16.08\pm1.80\,mm^3$, $n=29$). The infarct volume reduction was not significantly different between males and females, and the heterozygous females displayed an intermediate reduction, indicating a clear dose–response relation between relative AIF deficiency and infarct volume reduction (Figure 2b). Neuropathological scores were reduced in the cortex and hippocampus of both male and female Hq mice compared with their controls (Figure 2c). The striatum was significantly protected only in female Hq mice, and the thalamus only in males, but the overall score reduction was the same for males and females (Figure 2c).

Neither calpain nor caspase-3 activation was altered after HI in Hq mice. Immunoblots of cortex homogenates revealed fodrin degradation in the ipsilateral hemisphere 24 h after HI. The abundance of fodrin fragments generated by calpain activation (145 and 150 kDa) and caspase-3 activation (120 kDa) was the same for Hq and Wt mice (Figure 3a), suggesting that the AIF deficiency did not affect calpain or caspase activation after HI. Accordingly, homogenates from the damaged hemisphere contained similar activities capable of cleaving the caspase-3 substrate Ac-DEVD-aminomethyl-coumarin (AMC) both 3 and 24 h after HI (Figure 3b). Furthermore, release of cytochrome *c* from the mitochondrial fraction after HI was not different in Wt and Hq mice (not shown).

Caspase inhibition was equally protective in Wt and Hq mice. Five different caspase activities assayed 24 h post-HI were all significantly decreased after treatment with the broad-spectrum caspase inhibitor quinoline-Val-Asp(OMe)-CH_2-PH (Q-VD-OPh), verifying the efficacy of the inhibitor in this paradigm. Male Hq mutant pups treated with the caspase inhibitor ($n=7$) displayed significantly lower activities of caspase-1 (26.5%, $P=0.0157$), caspase-2 (58.8%, $P=0.0121$), caspase-3 (57%, $P=0.0054$), caspase-8 (35.8%, $P=0.0159$) and caspase-9 (48.3%, $P=0.0111$), as compared with vehicle-only treated animals ($n=8$) (Figure 4a). Q-VD-OPh administration also inhibited caspase-induced cleavage of fodrin (the 120 kDa fragment), but not oxidative stress, as judged by the nitrosylation of albumin (Figure 4b). Administration of Q-VD-OPh significantly reduced the brain infarct volume, both in Wt and in Hq mice, by a similar percentage (48 and 47%, respectively) (Figure 4c). Neuropathological scores also decreased significantly after Q-Vd-OPh administration, both in Wt and Hq pups (Figure 4d).

Hq mice benefited more than Wt mice from free radical scavenging. Treatment with the free radical scavenger edaravone, as described in Materials and Methods, did neither affect any of the five different caspase activities assayed 24 h post-HI (Figure 5a) nor did it change the levels of the caspase-induced 120 kDa fodrin fragment (Figure 5b). The average brain infarct volume was marginally reduced (24.8%) after edaravone treatment ($n=17$) compared with vehicle treatment ($n=16$) in Wt mice ($P=0.2$). In Hq mice, the infarct volume was reduced by 52.8% after edaravone treatment ($n=16$) as compared with vehicle treatment ($n=17$) ($P<0.001$) (Figure 5c). Neuropathological scores were significantly reduced in all brain regions in the Hq mutants after edaravone treatment, but in the Wt littermates a significant reduction was only seen in the striatum (Figure 5d).

After HI, there was a dramatic ($P<0.001$, not shown) increase in nitrotyrosine-positive cells in the ischemic brain areas (>10 cells/visual field in the cortex). This increase was particularly pronounced in Hq mice, where the increase was nearly twice as high as in Wt mice 3 h post-HI ($P<0.05$) (Figure 6a and b), and this increase was significantly ($P<0.001$) blunted by edaravone treatment in Hq but not in Wt mice (Figure 6a and b). Very similar results were obtained when nitrosylation was determined by immunoblotting. The brains of Hq mice exhibited more pronounced albumin nitrosylation in the infarcted area compared with Wt brains, and this was abolished by treatment with edaravone (Figure 6c). To obtain further information on the impact of the Hq mutation on oxidative stress, we also evaluated lipid peroxidation by immunostaining with an antibody specific for 4-hydroxy-2-nonenal (4-HNE). Very few cells from non-ischemic tissue of Hq or Wt mice were immunopositive (data not shown). However, after HI, 4-HNE-positive cells were abundant within the damaged area, and edaravone significantly reduced the frequency of 4-HNE-positive cells in Hq brains but not in Wt brains (Figure 6d and e).

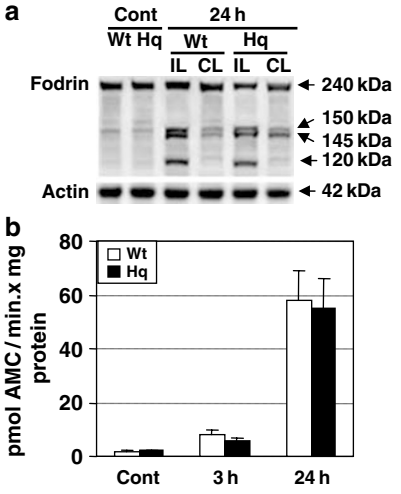

Figure 3 HI-induced caspase activation in Hq and Wt mice. (**a**) Representative fodrin immunoblots of cortex homogenates from naïve P9 non-ischemic controls (Cont) and homogenates obtained 24 h post-HI from the ipsilateral (IL) and contralateral (CL) hemispheres ($n=6$/group). Quantification of the caspase-dependent 120 kDa degradation product and the calpain-dependent 145/150 kDa degradation products revealed no significant differences between Wt and Hq mice (not shown). (**b**) Caspase-3-like activity (DEVD cleavage) measured in cortical homogenates from naïve P9 non-ischemic controls (Cont) and 3 or 24 h post-HI ($n=6$/group) in Wt and Hq mice. Data are means $\pm$ S.E.M.

Discussion

We demonstrate here for the first time that relative AIF deficiency is neuroprotective in a model of HI in the developing brain. The degree of protection is impressive, more than 50%, and the protection is more pronounced in the developing brain

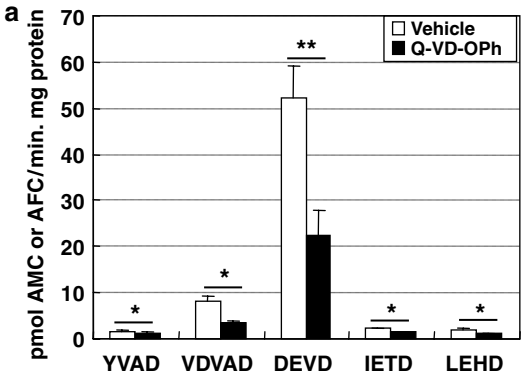

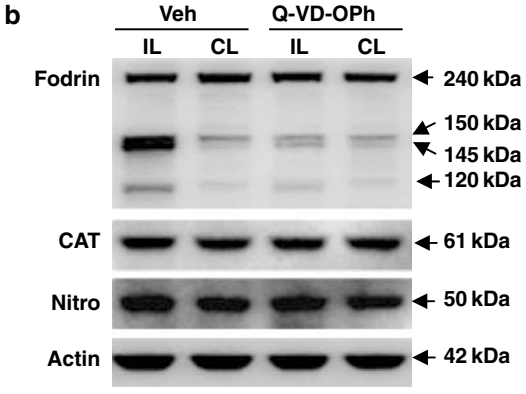

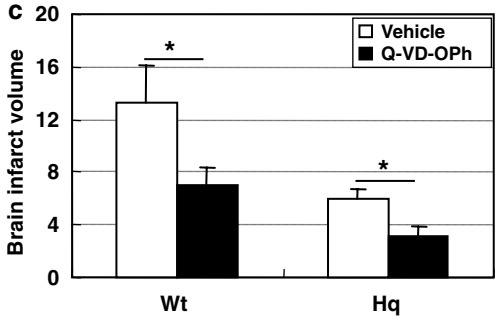

d

Groups	No.	Cortex	Hippocampus	Striatum	Thalamus	Total
Wt-Veh	n = 13	2.31 ± 0.33	3.44 ± 0.19	3.08 ± 0.22	1.77 ± 0.22	10.60 ± 0.78
Wt-Q-VD	n = 14	1.07 ± 0.35*	2.86 ± 0.32	1.84 ± 0.40*	0.93 ± 0.27*	6.70 ± 1.26*
Hq-Veh	n = 13	1.13 ± 0.25	3.02 ± 0.39	2.65 ± 0.39	1.42 ± 0.28	8.23 ± 1.22
Hq-Q-VD	n = 11	0.43 ± 0.18*	1.64 ± 0.3*	1.07 ± 0.33**	0.59 ± 0.24*	3.73 ± 0.93**

Figure 4 Effects of caspase inhibition on caspase activation and brain injury. (**a**) Caspase activities induced by HI and their inhibition by Q-VD-OPh. Fluorogenic peptide substrates were incubated with cortical tissue samples from male Hq brains 24 h post-HI. The peptides used were: YVAD, VDVAD, DEVD, IETD and LEHD, which are *bona fide* substrates of caspases-1, -2, -3, -8 and -9, respectively. Samples from mice treated with either vehicle ($n = 8$) or the broad-spectrum caspase inhibitor Q-VD-OPh ($n = 7$) were assayed for their ability to cleave the substrates, and all activities were significantly decreased in the Q-VD-OPh-treated animals. (**b**) Representative fodrin, catalase (CAT) and nitrotyrosine (Nitro) immunoblots of cortex homogenates from male P9 Hq mice treated with Q-VD-OPh or vehicle, obtained 24 h post-HI from the ipsilateral (IL) and contralateral (CL) hemispheres ($n = 6$/group). Actin was used for control of equal loading. (**c**) Infarct volumes observed in Wt and Hq mice treated with vehicle or Q-VD-OPh, 72 h after HI. Results are means ± S.E.M. (**d**) Neuropathological scores in various brain regions, as determined 3 days post-HI. The data presented represent the means ± S.E.M. $^*P < 0.05$, $^{**}P < 0.01$

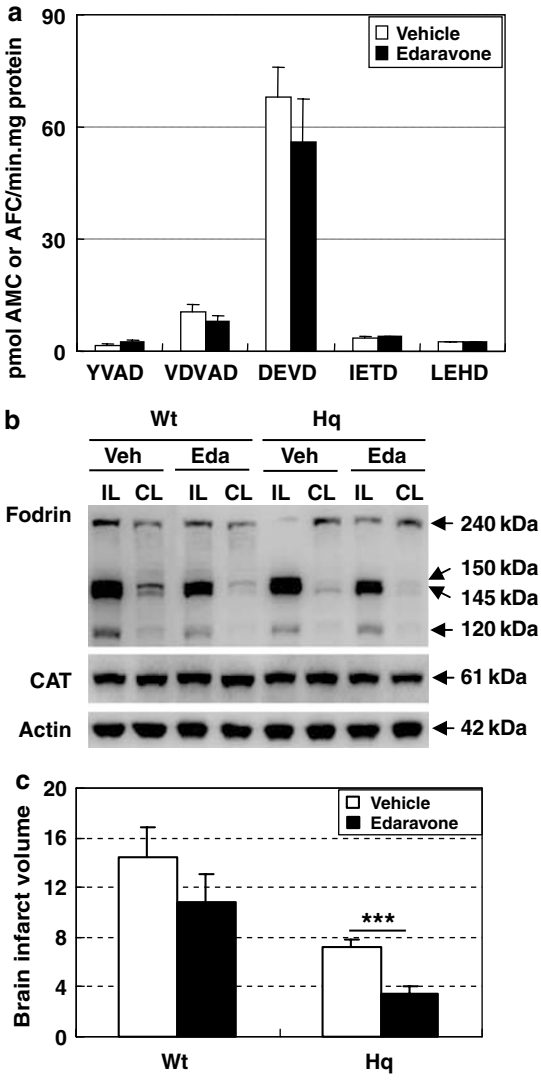

d

Groups	No.	Cortex	Hippocampus	Striatum	Thalamus	Total
Wt-Veh	n = 16	2.84 ± 0.27	3.31 ± 0.21	3.22 ± 0.19	1.92 ± 0.22	11.30 ± 0.75
Wt-Eda	n = 17	1.93 ± 0.37	2.81 ± 0.33	2.18 ± 0.36*	1.46 ± 0.27	8.37 ± 1.26
Hq-Veh	n = 17	1.69 ± 0.18	3.59 ± 0.23	3.16 ± 0.22	1.75 ± 0.19	10.19 ± 0.63
Hq-Eda	n = 16	0.61 ± 0.19***	2.20 ± 0.26***	1.38 ± 0.31***	0.80 ± 0.23**	4.98 ± 0.91***

Figure 5 Effects of edaravone on brain injury. (**a**) Caspase activities induced by HI and the effects of edaravone. Fluorogenic peptide substrates were incubated with cortical tissue samples from male Hq brains 24 h post-HI. The peptides used were: YVAD, VDVAD, DEVD, IETD and LEHD, which are *bona fide* substrates of caspases-1, -2, -3, -8 and -9, respectively. Samples from mice treated with either vehicle ($n = 8$) or edaravone ($n = 5$) were assayed for their ability to cleave the substrates, but none of the activities were significantly decreased in the edaravone-treated animals. (**b**) Representative fodrin and catalase (CAT) immunoblots of cortex homogenates from male P9 Hq mice treated with edaravone or vehicle, obtained 24 h post-HI from the ipsilateral (IL) and contralateral (CL) hemispheres ($n = 6$/group). Actin was used for control of equal loading. (**c**) Effects of edaravone treatment on brain infarct. Data are means ± S.E.M. (**d**) Neuropathological scores in various brain regions, as determined 3 days post-HI. The data presented represent the means ± S.E.M. $^{*}P < 0.05$, $^{**}P < 0.01$, $^{***}P < 0.001$

after HI than in the adult brain after focal ischemia,[16] despite our finding that AIF was more strongly downregulated in the adult brain, four-fold compared with 2.5-fold in the developing brain. This downregulation is in the same range as those reported earlier for adult Hq mice,[17] but the developmental difference in AIF deficiency in Hq mice has not shown before. Altogether, these findings underscore the contribution of AIF to neuronal demise induced by HI.

Amelioration of the neuroprotective effect of the Hq mutation by caspase inhibition. Our findings indicate that AIF and caspases act in parallel pathways leading to neuronal demise in the developing brain after HI. In molecular terms, AIF has been shown to induce caspase activation, either by contributing to the mitochondrial release of cytochrome *c*[12] or by sequestering HSP70, an inhibitor of apoptosome formation.[26] The levels of caspase-3-like activity were the same in Wt and Hq mice after HI, despite the fact that the infarcts were twice as large in the Wt mice. Caspase-3 is the most abundant effector caspase in the developing brain and it has been shown that there is a direct correlation between caspase-3 activation and the degree of injury after HI.[1–3,8,29] In light of this, it is surprising that Hq mice, displaying half the injury, still have the same levels of caspase-3 activation. It is unlikely that this can be explained by a delay in activation, because the caspase-3 activity was virtually identical in Wt and Hq mice both 3 and 24 h after HI. Also, the combined protective effect of the Hq mutation and caspase inhibition was no less than approximately 75% (Figure 4c). These results suggest that AIF and caspases act in parallel, non-overlapping pathways to mediate the HI-induced neuropathology, further indicating that the Hq mutation and caspase inhibition exert additive neuroprotective effects in neonatal HI.

Amelioraton of the neuroprotective effect of the Hq mutation by free radical scavenging. The AIF deficiency conferred by the Hq mutation reduces the anti-oxidant defense of neurons, thereby enhancing their susceptibility to oxidative stress.[17] This likely compromises the neuroprotective effect of the Hq mutation, because uncontrolled oxidative processes are thought to contribute to the acute neuronal loss induced by ischemia, particularly in the developing brain.[30] We therefore explored the possibility that reduction of oxidative stress through free radical scavenging might palliate the unwarranted side effects of AIF depletion, thereby increasing the therapeutic benefit conferred by the Hq mutation. Edaravone is a free radical scavenger that improves the outcome after cerebral ischemia in humans and is used for treatment after acute stroke.[31] Edaravone reportedly inhibits lipid peroxidation and scavenges nitric oxide and peroxynitrite.[32] We demonstrate that the combined effect of the Hq mutation and edaravone allowed a reduction in the overall brain infarct volume by approximately 75% compared with vehicle-treated Wt mice (Figure 5c). Altogether, these results suggest that edaravone ameliorates the neuroprotective effect of the Hq mutation, presumably by restoring the anti-oxidant defense compromised by the Hq mutation.

AIF is a suitable target for neuroprotective strategies. In this study, we addressed the question whether AIF might be a suitable therapeutic target for the treatment of cerebral

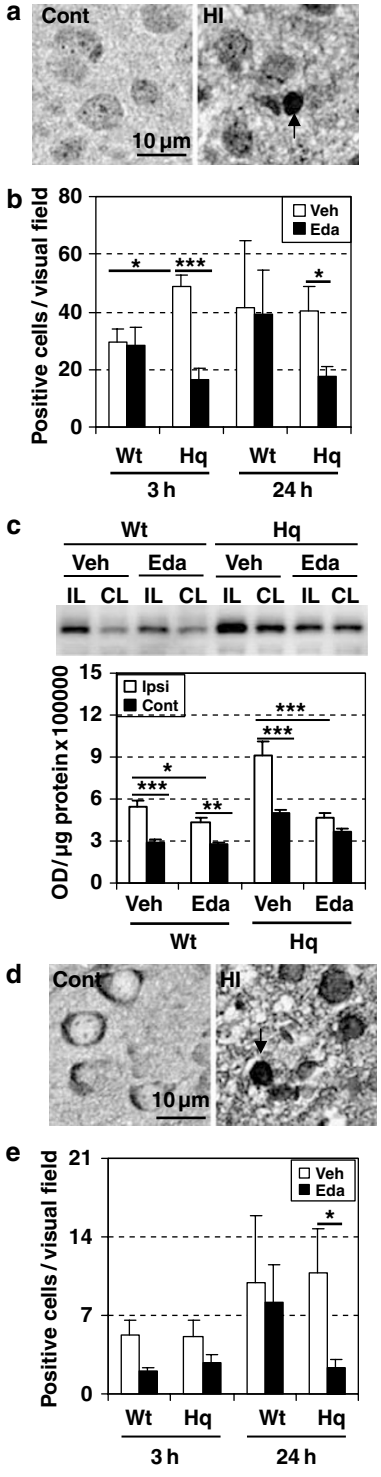

Figure 6 Formation of nitrotyrosine and 4-HNE in the cortex after HI. (**a**) Representative nitrotyrosine stainings in control and post-HI cortical tissue from Wt mice. A positive cell is indicated by an arrow in the right panel. (**b**) Nitrotyrosine-positive cells were counted in the cortex 3 and 24 h post-HI in male Wt and Hq mice after vehicle or edaravone treatment ($n = 6$/group). (**c**) Representative immunoblots of nitrosylated albumin (50 kDa) in cortical homogenates 24 h post-HI from male Wt ($n = 5$/group) and Hq mutant mice ($n = 7$/group) after treatment with vehicle or edaravone. Quantification of the optical densitometry is shown in the lower panel. (**d**) Representative 4-HNE stainings in control and post-HI cortical tissue from Wt mice. The arrow indicates a positive cell. (**e**) Cells positive for 4-HNE were counted in the cortex in Wt and Hq mice after treatment with vehicle or edaravone 3 and 24 h after HI. Results are means $\pm$ S.E.M. $^*P<0.05$, $^{**}P<0.01$, $^{***}P<0.001$. Scale bar $= 10\ \mu$m

ischemia. As mentioned in the Introduction, AIF has a dual function, first as a redox-active mitochondrial enzyme that assures an optimal oxidative phosphorylation and detoxification of ROS and, second, as a proapoptotic death effector that stimulates plasma membrane phosphatidylserine exposure and participates in chromatin condensation and apoptotic chromatinolysis. An ideal strategy would consist of inhibition of the proapoptotic activity of AIF without interfering with its implication in bioenergetic and redox metabolism. Unfortunately, no small inhibitory components that would selectively target the proapoptotic function of AIF are available thus far and current therapeutic strategies must rely on antisense constructs or siRNAs designed to downmodulate AIF expression[16] or by overexpressing AIF antagonists such as HSP70, which does provide a significant neuroprotective effect.[25] Here, we took advantage of the Hq mutation, which leads to a major reduction in AIF protein expression, to explore the contribution of AIF to neonatal brain damage inflicted by HI. The Hq mutation profoundly and significantly reduced the post-HI infarct volume, supporting a major role for AIF in the development of brain injury after ischemia. When the Hq mutation was combined with an anti-oxidant agent, the free radical scavenger edaravone, the infarct volume was strongly reduced by approximately 75%, whereas edaravone alone, in normal, AIF-expressing mice, had only a minor impact ($\sim$20% reduction in infarct volume, nonsignificant). These results correlated with the capacity of edaravone to suppress signs of oxidative damage in the infracted brain areas and these effects were particularly evident in Hq mice, suggesting that edaravone indeed compensated for the increased susceptibility to oxidative damage of neurons resulting from the hypomorphic AIF mutation. This may provide the theoretical framework to explain why the combination of AIF deficiency and edaravone exhibited a clearly hyperadditive therapeutic effect on neonatal brain damage after HI in Hq mice.

We also investigated the possibility to combine a lack of AIF, a quintessential caspase-independent death effector, with caspase inhibition using a broad-spectrum caspase inhibitor, Q-VD-OPh. Administration of Q-VD-OPh reduced the infarct volume in AIF-sufficient Wt mice and in AIF-deficient Hq mice, in both cases by approximately 50%. These data indicate that interruption of the caspase cascade and inhibition of AIF have an additive therapeutic effect leading to approximately 75% reduction of the infarct volume. The fact that these effects are simply additive suggests that the caspase activation pathway and the AIF pathway do not intersect, as has been found in some systems.[10] Accordingly, there was no difference in the level of caspase activation in Wt and Hq mice, again indicating that the level of AIF expression had no impact on the level of caspase activation. Thus, these data support a combination therapy in which both the caspase-dependent and the caspase-independent effector arms of the apoptotic machinery should be targeted simultaneously for an optimal clinical outcome.

In conclusion, our results delineate two distinct strategies for improving the therapeutic benefits of AIF inhibition. On the one hand, we suggest a method for antagonizing the counterproductive side effect of AIF depletion linked to an increased oxidative damage of the brain, namely the systematic application of the free radical scavenger edaravone. On the other hand, we demonstrate that the combination of AIF depletion and caspase inhibition has additive neuroprotective effects *in vivo*, in a model of neonatal brain ischemia.

Materials and Methods

Hypoxia-ischemia. Hq mice and their Wt or heterozygous littermates (The Jackson Laboratory, Bar Harbor, ME, USA) were subjected to transient, unilateral HI on P9, essentially according to the Rice–Vannucci model.[3,33] Mice were anesthetized with halothane (3.0% for induction and 1.0–1.5% for maintenance) in a mixture of nitrous oxide and oxygen (1 : 1), and the duration of anesthesia was $<$5 min. The left common carotid artery was cut between double ligatures of prolene sutures (6–0). After surgery, the wounds were infiltrated with a local anesthetic, and the pups were allowed to recover for 1–1.5 h. The litters were placed in a chamber perfused with a humidified gas mixture (10% oxygen in nitrogen) for 45 min. The temperature was kept at 36°C in the incubator and in the water used to humidify the gas mixture. After hypoxic exposure, the pups were returned to their biological dams until killed. All animal experimental protocols were approved by the Göteborg committee of the Swedish Animal Welfare Agency (94-2003 and 184-2003).

Genotyping and sex identification by PCR. Genomic DNA was isolated from tail samples. The tail was digested with 400 μl lysis buffer (50 mM Tris-HCl, pH 8.0, 100 mM EDTA, 100 mM NaCl, 1% SDS) containing 1 mg/ml proteinase K (Roche). Following incubation at 60°C overnight, 200 μl 5 M potassium acetate was added to the lysate which was thoroughly mixed and centrifuged at 10 000 $\times$ *g* for 20 min. The supernatant was transferred into a clean tube and 800 μl 100% ethanol was added and mixed. After incubation at $-$20°C for 30 min, the DNA was pelleted by centrifugation at 10 000 $\times$ *g* for 25 min at 4°C. The pellet was washed once with 500 μl 75% ethanol. The pellet was dried and subsequently dissolved in 50 μl sterile water and the DNA concentration was determined.

The reaction mixture for genotyping contained 1 μl of genomic DNA, 0.2 mM dNTP, 2.5 μl 10 $\times$ PCR buffer (250 mM Tris-HCl, pH 8.3, 375 mM KCl, 15 mM MgCl2, Sigma), 1 U of Taq DNA polymerase (Sigma), either 0.5 μM of Hq common and Hq Wt primers or 0.5 μM of Hq common and 0.5 μM Hq mutant primer. The PCR cycles were 94°C for 45 s, 60°C for 45 and 72°C for 1 min over 35 cycles. The following primers were used: Hq common: 5′-CTA TGC CCT TCT CCA TGT AGT T-3′, Hq Wt: 5′-AGT GTC CAG TCA AAG TAC CGG G-3′ and Hq mutant: 5′-CCA GAA ACT GTC TCA AGG TTC C-3′. PCR products were separated on a 1.5% agarose gel containing 0.5 μg/ml ethidium bromide. A 100-base pair (bp) ladder was used to verify the size of the PCR products. The gels were exposed in a LAS 3000 cooled CCD camera (Fujifilm, Tokyo, Japan). Hq mutant mice were identified by the presence of a single 500 bp DNA band. Wt mice were identified by a single 520 bp product. Heterozygous females showed both 520 and 500 bp bands.

The sex identification was performed as described previously.[34] The mouse SRY gene primers were used for PCR (forward primer: 5′-ATC TTA GAG AGA CAG GAG AGC AG-3′, reverse primer: 5′-TGA CTA ATC ACC ACC TGG TAG CT-3′). Males were identified by the presence of a single 335 bp band.

Blood analysis. P9 animals of Wt ($n=8$) and Hq mutant mice ($n=6$) were decapitated and mixed arterial and venous blood was collected in a capillary tube from the neck vessels. Blood pH, P_{CO2}, glucose (Glu), lactate (Lac) and bicarbonate (HCO_3) were analyzed immediately in a blood analyzer (ABL 725, Radio meter A/S, Copenhagen, Denmark).

Caspase inhibition. The broad-spectrum caspase inhibitor Q-VD-OPH (Enzyme Systems Products, Livermore, CA, USA) was dissolved in 100% DMSO and diluted with saline. It was injected twice intraperitoneally at a dose of 10 mg/kg (10 μl/g body weight), immediately after artery occlusion and immediately after hypoxia. Control pups received an equivalent volume of saline containing 10% DMSO.

Oxidative stress inhibition. The free radical scavenger edaravone (3-methyl-1-phenyl-2-pyrazolin-5-one, MCI-186 from BIOMOL, Plymouth Meeting, PA, USA) was dissolved in 100% DMSO and diluted with saline. It was injected twice

intraperitoneally at a dose of 10 mg/kg (10 μl/g body weight), immediately after artery occlusion and immediately after hypoxia. Control groups received an equivalent volume of saline containing 10% DMSO.

Tissue preparation. Pups were deeply anaesthetized with 50 mg/ml phenobarbital at 3, 24 or 72 h after HI. Control animals were killed on P9. The brains were perfusion fixed with 5% formaldehyde in 0.1 M phosphate buffer through the ascending aorta for 5 min. The brains were rapidly removed and immersion-fixed at 4°C for 24 h. The brains were dehydrated with xylene and graded ethanol, paraffin-embedded and serial cut into 5 μm frontal sections. Deparaffinized sections were used for nitrotyrosine, 4-HNE and MAP2 immunostaining as described below.

Gene expression analysis. Brains from P9 Wt ($n=5$) and Hq ($n=5$) male pups were frozen in liquid nitrogen. Total forebrain RNA was isolated and Affymetrix array expression was performed at the Swegene facility in Lund, Sweden, using MOE430 2.0 chips. Log-transformed, normalized data were analyzed using the GeneSifter software (VizX Labs, Seattle, WA, USA) with Benjamini Hochberg correction.

Sample preparation for immunoblotting. Animals were killed by decapitation 3 or 24 h after HI. Control animals were killed on P9. The brains were rapidly dissected out on a bed of ice. The parietal cortex (including the hippocampus) was dissected out from each hemisphere and ice-cold isolation buffer was added (15 mM Tris-HCl, pH 7.6, 320 mM sucrose, 1 mM DTT, 1 mM $MgCl_2$, 3 mM EDTA-K, 0.5% protease inhibitor cocktail (P8340; Sigma) and 2.5 μM cyclosporin A. Homogenization was performed gently by hand (to preserve mitochondrial integrity) in a 2 ml glass/glass homogenizer (Merck Euro lab, Dorset, England) using, sequentially, two different pestles with a total clearance of 0.12 and 0.05 mm, respectively (10 strokes each). The homogenates were centrifuged at $800 \times g$ for 10 min at 4°C. The pellets were washed in homogenizing buffer and recentrifuged at $800 \times g$ for 15 min at 4°C, producing a crude nuclear pellet (P1). The supernatant from the first centrifugation was further centrifuged at $9200 \times g$ for 15 min at 4°C, producing a mitochondrial and synaptosomal fraction in the pellet (P2) and a crude cytosolic fraction in the supernatant (S2). All fractions were stored at −80°C.

Immunohistochemistry. Antigen recovery was performed by heating the sections in 10 mM boiling sodium citrate buffer (pH 6.0) for 10 min. Nonspecific binding was blocked for 30 min with 4% horse or goat serum (depending on the species used to raise the secondary antibody) in phosphate-buffered saline. Anti-nitrotyrosine (1 : 100, 10 μg/ml, A-21285, Molecular probes, Eugene, OR, USA), anti-4-HNE (1 : 500, HNE11-S, Alpha Diagnostic International, San Antonio, USA) and anti-MAP2 (1 : 1000, clone HM-2, Sigma) were incubated for 60 min at room temperature, followed by the appropriate, biotinylated goat anti-rabbit (1 : 150, for nitrotyrosine and 4-HNE, Vector, Burlingame, CA) or biotinylated horse anti-mouse (1 : 200, for MAP2, Vector, Burlingame, CA, USA) secondary antibody for 60 min at room temperature. Endogenous peroxidase activity was blocked with 3% H_2O_2 for 5 min. Visualization was performed using Vectastain ABC Elite with 0.5 mg/ml 3,3′-diaminobenzidine enhanced with 15 mg/ml ammonium nickel sulfate, 2 mg/ml β-D-Glu, 0.4 mg/ml ammonium chloride and 0.01 mg/ml β-Glu oxidase (all from Sigma).

Immunoblotting. The protein concentrations were determined according to Whitaker and Granum,[35] adapted for microplates. Samples of 65 μl were mixed with 25 μl NuPAGE LDS 4 × sample buffer and 10 μl reducing agent and heated (70°C) for 10 min. Individual samples were run on 4–12% NuPAGE Bis-Tris gels (Novex, San Diego, CA, USA) and transferred to reinforced nitrocellulose membranes (Schleicher & Schuell, Dassel, Germany). After blocking with 30 mM Tris-HCl (pH 7.5), 100 mM NaCl and 0.1% Tween 20 (TBS-T) containing 5% fat-free milk powder for 1 h at room temperature, the membranes were incubated with primary antibodies: anti-AIF (sc-9416, 1 : 1000, 0.2 μg/ml, goat polyclonal antibody, Santa Cruz, CA, USA), anti-caspase-3 (H-277, 1 : 1000, rabbit polyclonal antibody, Santa Cruz, CA, USA), anti-cytochrome *c* (1 : 500, clone 7H8.2C12, Pharmingen, San Diego, CA, USA), anti-actin (1 : 200, rabbit polyclonal antibody, A2066, Sigma, Stockholm, Sweden), anti-superoxide dismutase I (Cu,Zn-SOD/SOD1, 1 : 2000, 0.5 μg/ml, rabbit polyclonal antibody, Lab Frontier, Seoul, Korea), anti-superoxide dismutase II (Mn-SOD/SOD2, 1 : 1000, 0.5 μg/ml, clone 2A1, Lab Frontier, Seoul, Korea), anti-fodrin (1 : 500, 0.2 μg/ml, clone AA6, BIOMOL, Plymouth Meeting, PA, USA), anti-nitrotyrosine (1 μg/ml, HM12, BIOMOL, Plymouth Meeting, PA, USA), anti-catalase (1 : 250, 1 μg/ml, clone 11A1, Lab Frontier, Seoul, Korea), anti-TRX2 (1 : 1000, 1 μg/ml, rabbit polyclonal antibody, Lab Frontier, Seoul, Korea), anti-OxPhos Complex I 39 kDa subunit (1 : 1000, 0.5 μg/ml, p39, clone 20C11, Molecular probes, Eugene, OR, USA), anti-PARP (1 : 1000, clone C-2-10, ZYMED Laboratories, South San Francisco, CA, USA), at room temperature for 60 min. After washing, the membranes were incubated with a peroxidase-labeled secondary antibody for 30 min at room temperature (goat anti-rabbit, 1 : 2000, horse anti-goat, 1 : 2000 or horse anti-mouse 1 : 4000). Immunoreactive species were visualized using the Super Signal West Dura substrate (Pierce, Rockford, IL, USA) and a LAS 3000 cooled CCD camera (Fujifilm, Tokyo, Japan).

Caspase activity assays. The protein concentrations were determined as above. Samples of homogenate (25 μl) were mixed with 75 μl of extraction buffer as described earlier.[3] Cleavage of Ac-YVAD-AMC (for caspase-1, from Alexis Corp., San Diego, CA, USA), Ac-DEVD-AMC (for caspase-3, Peptide Institute, Osaka, Japan), was measured with an excitation wavelength of 380 nm and an emission wavelength of 460 nm, and expressed as pmol AMC released per mg protein and minute. Cleavage of Ac-VDVAD-AFC (for caspase-2), Ac-IETD-AFC (for caspase-8) and Ac-LEHD (for caspase-9) (all AFC substrates were from Enzyme System Products, Livemore, CA, USA) was measured as for the AMC conjugates, but with an excitation wavelength of 400 nm and an emission wavelength of 505 nm, and expressed as pmol AFC released per mg protein and minute.

Injury evaluation

Neuropathological scoring. Brain injury at 72 h post-HI in different regions was evaluated using a semiquantitative neuropathological scoring system as described earlier.[8] Briefly, sections were stained for MAP2 and scored by an observer blinded to the treatment of the animals. The cortical injury was graded from 0 to 4, 0 being no observable injury and 4 confluent infarction encompassing most of the cerebral cortex. The damage in hippocampus, striatum and thalamus was assessed both with respect to hypotrophy (shrinkage) (0–3) and observable cell injury/infarction (0–3) resulting in a neuropathological score for each brain region (0–6). The total score (0–22) was the sum of the scores for all four regions.

Tissue volume. The infarct volumes were measured at 72 h post-HI by sectioning the entire brains into 5 μm sections and staining every 100th section for MAP2. The loss of MAP2 staining in the cortex, striatum, thalamus and hypothalamus was measured using Micro Image (Olympus, Japan) and the volumes calculated according to the Cavalieri Principle using the following formula: $V=\sum A \times P \times T$, where V = total volume, $\sum A$ is the sum of the areas measured, P is the inverse of the sampling fraction and T is the section thickness.

Cell counting. Cell counting was performed in the cortex of ipsilateral hemispheres and P9 controls. Positive cells were counted at × 400 magnification (one visual field = 0.196 mm^2). Three visual fields in the infarct border zone were counted and expressed as average number per visual field.

Statistics. All data were expressed as mean ± S.E.M. Student's *t*-test was used when comparing injury scores, tissue loss or the numbers of immunopositive cells between two different groups. ANOVA with Fisher's *post hoc* test was used when comparing more than two groups. Significance level was assigned at $P<0.05$.

Acknowledgements. This work was supported by the Swedish Research Council, the Swedish Child Cancer Foundation (Barncancerfonden, to KB), Swedish governmental grants to scientists working in health care (ALF), the National Natural Science Foundation of China (to CZ), EU grants (Trans-Death, to GK), the Åhlén Foundation, the Wilhelm and Martina Lundgren Foundation, the Magnus Bergvall Foundation, the Frimurare Barnhus Foundation, the Göteborg Medical Society and the Swedish Society of Medicine.

1. Blomgren K, Zhu C, Wang X, Karlsson JO, Leverin AL, Bahr BA *et al.* Synergistic activation of caspase-3 by m-calpain after neonatal hypoxia-ischemia: a mechanism of 'pathological apoptosis'? *J Biol Chem* 2001; **276**: 10191–10198.
2. Hu BR, Liu CL, Ouyang Y, Blomgren K, Siesjo BK. Involvement of caspase-3 in cell death after hypoxia-ischemia declines during brain maturation. *J Cereb Blood Flow Metab* 2000; **20**: 1294–1300.
3. Zhu C, Wang X, Xu F, Bahr BA, Shibata M, Uchiyama Y *et al.* The influence of age on apoptotic and other mechanisms of cell death after cerebral hypoxia-ischemia. *Cell Death Differ* 2005; **12**: 162–176.

4. Friberg H, Ferrand-Drake M, Bengtsson F, Halestrap AP, Wieloch T, Cyclosporin A. but not FK 506, protects mitochondria and neurons against hypoglycemic damage and implicates the mitochondrial permeability transition in cell death. *J Neurosci* 1998; **18**: 5151–5159.
5. Green DR, Kroemer G. The pathophysiology of mitochondrial cell death. *Science* 2004; **305**: 626–629.
6. Kluck RM, Esposti MD, Perkins G, Renken C, Kuwana T, Bossy-Wetzel E *et al.* The pro-apoptotic proteins, Bid and Bax, cause a limited permeabilization of the mitochondrial outer membrane that is enhanced by cytosol. *J Cell Biol* 1999; **147**: 809–822.
7. Spierings D, McStay G, Saleh M, Bender C, Chipuk J, Maurer U *et al.* Connected to death: the (unexpurgated) mitochondrial pathway of apoptosis. *Science* 2005; **310**: 66–67.
8. Wang X, Zhu C, Hagberg H, Korhonen L, Sandberg M, Lindholm D *et al.* X-linked inhibitor of apoptosis (XIAP) protein protects against caspase activation and tissue loss after neonatal hypoxia-ischemia. *Neurobiol Dis* 2004; **16**: 179–189.
9. Cheng Y, Deshmukh M, D'Costa A, Demaro JA, Gidday JM, Shah A *et al.* Caspase inhibitor affords neuroprotection with delayed administration in a rat model of neonatal hypoxic-ischemic brain injury. *J Clin Invest* 1998; **101**: 1992–1999.
10. Susin SA, Daugas E, Ravagnan L, Samejima K, Zamzami N, Loeffler M *et al.* Two distinct pathways leading to nuclear apoptosis. *J Exp Med* 2000; **192**: 571–580.
11. Yoshida H, Kong YY, Yoshida R, Elia AJ, Hakem A, Hakem R *et al.* Apaf1 is required for mitochondrial pathways of apoptosis and brain development. *Cell* 1998; **94**: 739–750.
12. Susin SA, Lorenzo HK, Zamzami N, Marzo I, Snow BE, Brothers GM *et al.* Molecular characterization of mitochondrial apoptosis-inducing factor. *Nature* 1999; **397**: 441–446.
13. Cheung EC, Melanson-Drapeau L, Cregan SP, Vanderluit JL, Ferguson KL, McIntosh WC *et al.* Apoptosis-inducing factor is a key factor in neuronal cell death propagated by BAX-dependent and BAX-independent mechanisms. *J Neurosci* 2005; **25**: 1324–1334.
14. Kroemer G, Martin SJ. Caspase-independent cell death. *Nat Med* 2005; **11**: 725–730.
15. Modjtahedi N, Giordanetto F, Madeo F, Kroemer G. Apoptosis-inducing factor: vital and lethal. *Trends Cell Biol* 2006; **16**: 264–272.
16. Culmsee C, Zhu C, Landshamer S, Becattini B, Wagner E, Pellechia M *et al.* Apoptosis-inducing factor triggered by poly(ADP-Ribose) polymerase and bid mediates neuronal cell death after oxygen-glucose deprivation and focal cerebral ischemia. *J Neurosci* 2005; **25**: 10262–10272.
17. Klein JA, Longo-Guess CM, Rossmann MP, Seburn KL, Hurd RE, Frankel WN *et al.* The harlequin mouse mutation downregulates apoptosis-inducing factor. *Nature* 2002; **419**: 367–374.
18. Vahsen N, Cande C, Briere JJ, Benit P, Joza N, Larochette N *et al.* AIF deficiency compromises oxidative phosphorylation. *EMBO J* 2004; **23**: 4679–4689.
19. Zhu C, Qiu L, Wang X, Hallin U, Cande C, Kroemer G *et al.* Involvement of apoptosis-inducing factor in neuronal death after hypoxia-ischemia in the neonatal rat brain. *J Neurochem* 2003; **86**: 306–317.
20. Plesnila N, Zhu C, Culmsee C, Groger M, Moskowitz MA, Blomgren K. Nuclear translocation of apoptosis-inducing factor after focal cerebral ischemia. *J Cereb Blood Flow Metab* 2004; **24**: 458–466.
21. Ferrand-Drake M, Zhu C, Gido G, Hansen AJ, Karlsson JO, Bahr BA *et al.* Cyclosporin A prevents calpain activation despite increased intracellular calcium concentrations, as well as translocation of apoptosis-inducing factor, cytochrome *c* and caspase-3 activation in neurons exposed to transient hypoglycemia. *J Neurochem* 2003; **85**: 1431–1442.
22. Fukuda H, Fukuda A, Zhu C, Korhonen L, Swanpalmer J, Hertzman S *et al.* Irradiation-induced progenitor cell death in the developing brain is resistant to erythropoietin treatment and caspase inhibition. *Cell Death Differ* 2004; **11**: 1166–1178.
23. Yu SW, Wang H, Poitras MF, Coombs C, Bowers WJ, Federoff HJ *et al.* Mediation of poly(ADP-ribose) polymerase-1-dependent cell death by apoptosis-inducing factor. *Science* 2002; **297**: 259–263.
24. Polster BM, Basanez G, Etxebarria A, Hardwick JM, Nicholls DG. Calpain I induces cleavage and release of apoptosis-inducing factor from isolated mitochondria. *J Biol Chem* 2005; **280**: 6447–6454.
25. Matsumori Y, Hong SM, Aoyama K, Fan Y, Kayama T, Sheldon RA *et al.* Hsp70 overexpression sequesters AIF and reduces neonatal hypoxic/ischemic brain injury. *J Cereb Blood Flow Metab* 2005; **25**: 899–910.
26. Ravagnan L, Gurbuxani S, Susin SA, Maisse C, Daugas E, Zamzami N *et al.* Heat-shock protein 70 antagonizes apoptosis-inducing factor. *Nat Cell Biol* 2001; **3**: 839–843.
27. Wang H, Yu SW, Koh DW, Lew J, Coombs C, Bowers W *et al.* Apoptosis-inducing factor substitutes for caspase executioners in NMDA-triggered excitotoxic neuronal death. *J Neurosci* 2004; **24**: 10963–10973.
28. Liou AK, Zhou Z, Pei W, Lim TM, Yin XM, Chen J. BimEL up-regulation potentiates AIF translocation and cell death in response to MPTP. *FASEB J* 2005; **19**: 1350–1352.
29. Zhu C, Wang X, Hagberg H, Blomgren K. Correlation between caspase-3 activation and three different markers of DNA damage in neonatal cerebral hypoxia-ischemia. *J Neurochem* 2000; **75**: 819–829.
30. Blomgren K, Hagberg H. Free radicals, mitochondria, and hypoxia-ischemia in the developing brain. *Free Radical Biol Med* 2006; **40**: 388–397.
31. Group, EAIS, Effect of a novel free radical scavenger, edaravone (MCI-186), on acute brain infarction. Randomized, placebo-controlled, double-blind study at multicenters. *Cerebrovasc Dis* 2003; **15**: 222–229.
32. Noor JI, Ikeda T, Mishima K, Aoo N, Ohta S, Egashira N *et al.* Short-term administration of a new free radical scavenger, edaravone, is more effective than its long-term administration for the treatment of neonatal hypoxic-ischemic encephalopathy. *Stroke* 2005; **36**: 2468–2474.
33. Rice III JE, Vannucci RC, Brierley JB. The influence of immaturity on hypoxic-ischemic brain damage in the rat. *Ann Neurol* 1981; **9**: 131–141.
34. Zhu C, Xu F, Wang X, Shibata M, Uchiyama Y, Blomgren K *et al.* Different apoptotic mechanisms are activated in male and female brains after neonatal hypoxia-ischaemia. *J Neurochem* 2006; **96**: 1016–1027.
35. Whitaker JR, Granum PE. An absolute method for protein determination based on difference in absorbance at 235 and 280 nm. *Anal Biochem* 1980; **109**: 156–159.

Supplementary Information accompanies the paper on Cell Death and Differentiation website (http://www.nature.com/cdd)